Parameter Studies for Spectral Imager Application Performance

John P. Kerekes
Rochester Institute of Technology
Chester F. Carlson Center for Imaging Science
54 Lomb Memorial Drive
Rochester, New York 14623 USA

Abstract—**Multi- and hyperspectral imaging systems have found utility in a variety of earth remote sensing applications. Much research has focused on developing new ways to process the data and obtain improved results in a given application. However, relatively little research has focused on the open question of what is the optimum performance possible in a given situation. The work discussed in this paper is aimed at exploring that question through analytical modeling and performance trade studies. We show example analysis results that indicate performance floors where no further improvement is possible due to improved spatial resolution or signal-to-noise ratios in given analysis tasks.**

Keywords-spectral imaging system modeling, multispectral, hyperspectral, target detection, classification, parameter studies

I. INTRODUCTION

Multi- and hyperspectral imaging systems have found utility in a variety of earth remote sensing applications. Unresolved object detection, land cover classification and geologic mineral identification are a few of the predominant tasks that have been demonstrated with spectral imagery. Many studies have been published which describe in great detail the accuracy and error rates associated with these tasks for a particular data set. Often the focus of these publications has been on how the authors' new algorithm outperforms existing community approaches. These efforts have benefited the community and led to new algorithms implemented in commercial analysis packages or made available through the Internet. Of course, as good as these algorithms are, the community continues to investigate new processing and exploitation approaches in the search of ever-more robust and automated tools.

While the pursuit of improved processing tools is certainly important and worthwhile, there has been relatively little research into the fundamental questions of how well can a given spectral imaging system perform a specific task and what aspects of the remote sensing process limit that performance. An accurate understanding and ability to predict performance for a given system would be very useful not only during the design and operation of the system, but could also possibly provide a metric for comparison when developing and evaluating new processing algorithms. For example, if a particular system could be shown to be capable of no more than 80% accuracy in a certain land cover classification problem because of the inherent spectral overlap of the classes and the sensor's measurement characteristics, and the common maximum likelihood classifier achieves 79%, then it likely would not make sense to embark on a research effort to develop new algorithms to gain that 1% in accuracy.

It has been this goal of understanding the possible performance and the role of parameters in a spectral imaging system that has motivated our research into modeling the remote sensing process [1], [2]. Of course, anyone with a modest familiarity with spectral imaging for earth remote sensing realizes the complexity and interdependency of the many aspects of the process. The characteristics of the scene, the analysis task at hand, the intervening atmosphere, the sensor, the processing and analysis algorithms, and even the analysts' expertise all affect the achievable performance. Thus, this task is very challenging and progress is likely to be made incrementally over time.

The Forecasting and Analysis of Spectroradiometric System Performance (FASSP) model was initially developed at MIT Lincoln Laboratory specifically to explore spectral imaging system performance and parameter sensitivity. It considers the remote sensing process as a linear system propagating surface class statistics through the system arriving at a measure of performance. The model theory, validation and example analyses have been described in the literature [3], [4].

This paper focuses on the use of the FASSP model in studying the relative importance of parameters of the remote sensing process in the application of unresolved target detection using hyperspectral imagery. Following a brief description of the FASSP model, we then describe the scenario analyzed. Results are then shown illustrating the quantitative performance sensitivity to parameter variation. Finally, we summarize and discuss the implications of these results in determining the most significant parameters.

II. ANALYTICAL END-TO-END SYSTEM MODEL

The analytical end-to-end performance prediction tool FASSP has been developed in support of hyperspectral imaging system design and analysis studies. One application of this tool has been to predict target detection performance for a specified scenario. Through the use of statistical descriptions for the target and background, and linear transformations to model the effects of the observing system and processing, the performance can be predicted analytically, rather than through a physics-based simulation. This approach runs very quickly and can efficiently support large numbers of trade studies.

The underlying premises of the FASSP model are 1) that the various surface classes and subclasses of interest can be represented by first- and second-order spectral statistics (and other parameters) and 2) that the effects of various processes in the end-to-end spectral imaging system can be modeled as transformations and functions of those statistics and parameters. The model propagates the spectral statistics through the effects of the atmosphere, the sensor, atmospheric compensation, feature extraction techniques, and then applies a detection algorithm to convert the high dimensional statistics to a scalar test statistic (matched filter output) to which a threshold can be applied and detection performance computed. Fig. 1 presents a block diagram of the model.

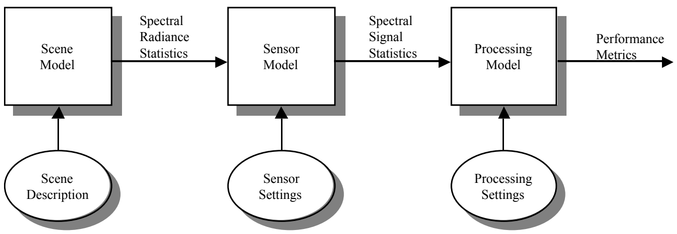

Figure 1. Block diagram of the FASSP model structure.

One application of the model is unresolved, or subpixel, target detection scenarios. Here the linear mixing model is used and the pixel of interest containing the target is assumed to be a sample from random process described by the area-weighted mixture of the target and the background classes. The rest of the analytically-described scene (no simulated "image" is generated by the model) is comprised of a number of homogeneous background classes, each covering an area percentage of the scene. The scene false alarm rate at a given threshold is then computed as the area-weighted total of false alarms from each individual background class.

While the initial version of the model computed these class-specific false alarm rates assuming a Gaussian distribution for the output of the matched filter detector, a recent enhancement generalized the form of the background distributions to the class of elliptically contoured distributions [5]. These distributions are characterized by their mean, covariance, and a degree-of-freedom parameter which controls the "heaviness" of the distribution tail. Large values of this parameter (> 25) lead to Gaussian distributions while small values (<10) have significantly longer tails. Since the tails of the distributions drive the false alarm rate, setting this parameter to the lower values allows the modeling of more challenging backgrounds for target detection applications.

III. Model Scenario

The scenario selected for analysis in this work is one of detecting particular civilian vehicles within a cluttered urban environment using hyperspectral imagery. This task is one aspect of "tracking" a given vehicle across sequential frames of imagery [6].

Table 1 presents the scenario parameters used in the model analyses. Five vehicle paint types were included in the scene (blue car 1, blue car 2, green car 1, green car 2, and white car). For each analysis, one was considered the "target" while the others were included in the scene as "background" classes (confusers) at 1% of the scene area. Fig. 2 shows the spectral mean reflectance of these vehicles as measured by a field spectrometer and used in the model. Note that estimates of the spectral covariance matrices for the various vehicle paints were also made from multiple measurements collected by the field spectrometer and used in the model.

TABLE I. Scenario Parameters

Parameter	Value(s)
Target	Blue car 1 (other cars studied as well)
Backgrounds	25% roadway, 15% grass, 15% trees, 15% roof 1, 10% roof 2, 10% bare ground, 5% water, 1% blue car 2, 1% green car 1, 1% green car 2, 1% white car
Visibility	10 km with rural aerosol model
Solar zenith angle	30°
Atmospheric model	Summer mid-latitude
Sensor altitude	3.1 km
Sensor	HYDICE
Atmospheric compensation	ELM
Detection algorithm	Spectral matched filter
Spectral channels used in filter	144 (64 in 0.42-0.90 μm, 16 in 1.10-1.32 μm, 16 in 1.53-1.72 μm, and 48 in 2.01-2.45 μm)

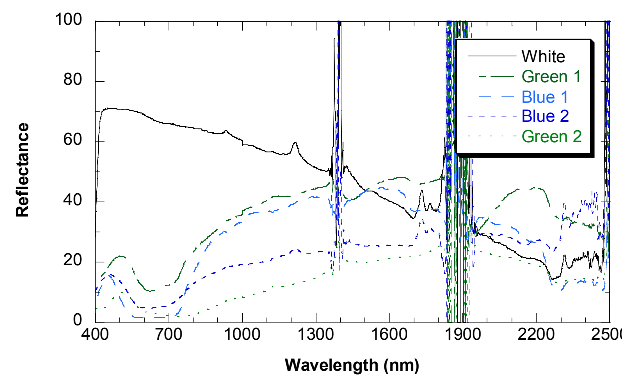

Figure 2. Vehicle mean reflectance.

The statistics for the background were obtained by atmospherically compensating airborne HYDICE [7] hyperspectral imagery collected over an urban area and classified into homogenous classes. A model of the HYDICE sensor was also implemented within FASSP and used in these analyses. Table 1 also indicates the other MODTRAN [8] atmospheric parameters used in the model and notes atmospheric compensation using the empirical line method (ELM) was applied before detection using a normalized spectral matched filter.

IV. Results

The first analysis conducted was to examine the receiver operating characteristic, or ROC curve, for the various vehicle paints in the given scenario. The vehicles were modeled such that they only filled 25% of the area of a ground pixel for the sensor, with the other 75% consisting of road background. This was done to achieve less than perfect detection given the other system parameters assumed. Fig. 3 presents the results.

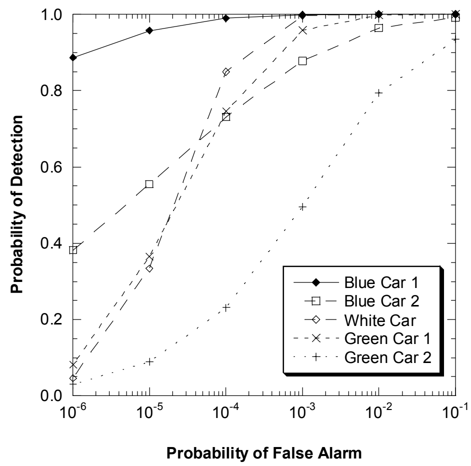

Figure 3. P_D vs. P_{FA} for vehicles occupying 25% of a pixel in scene with eleven class background, and SNR=100 with 144 spectral channels covering the VNIR and SWIR regions.

In Fig. 3 we see that the Blue Car 1 paint is the easiest to detect while the Green Car 2 paint was the most difficult. Referring back to Fig. 2, we can see the Blue 1 paint is fairly bright with distinctive spectral features while Green 2 is dark and more spectrally flat.

The analysis shown in Fig. 3 used the Gaussian assumption for the eleven background classes. For comparison, we predicted the ROC curve for Green Car 1 as the target against a single background (roadway) class modeled with an elliptical-t distribution with varying degrees-of-freedom (DOF) as noted in the legend of Fig. 4. Comparing Figs. 3 and 4, we see a single class elliptical-t background with DOF=6 leads to similar ROC curve performance as the eleven class Gaussian background. Fig. 4 also indicates the use of higher DOF's to model more complex background situations.

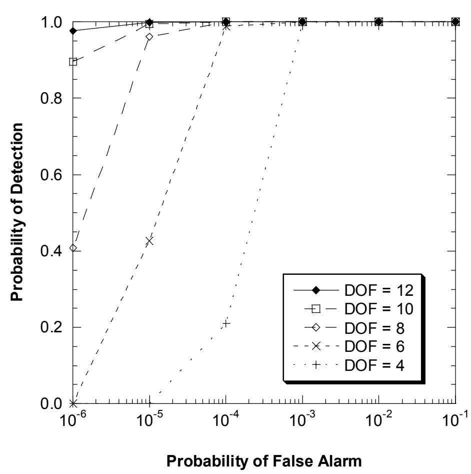

Figure 4. P_D vs. P_{FA} for Green Car 1 with same conditions as Fig. 3 except a single background (roadway) with an elliptical-T distribution with degrees of freedom as shown.

Next the relationship between subpixel fill fraction and sensor signal-to-noise ratio (SNR) was investigated. Fig. 5 plots detection probability vs. target subpixel fill fraction for Green Car 1 as a function of SNR. For these various SNR's, noise was added to the signals with a standard deviation equal to the inverse of the SNR times the signal level. This has the result of having a nearly constant SNR across the wavelengths. While this is not typically how real instruments perform, it is convenient for the trade study.

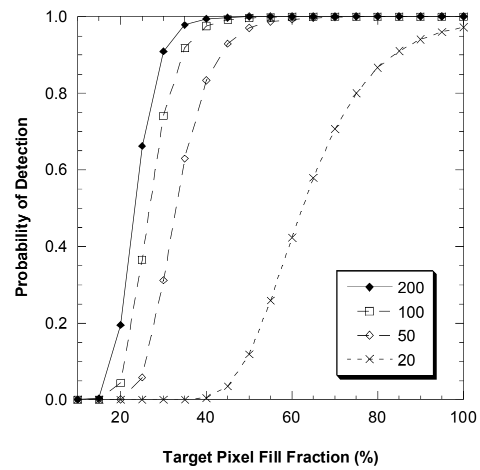

Figure 5. P_D (@$P_{FA} = 10^{-5}$) vs. target pixel fill fraction for Green Car 1 for various SNR's.

The results shown in Fig. 5 indicate detection is possible down to significantly smaller subpixel fractions at higher SNR levels. Since this result was just for the one vehicle paint type, it raises the question of how that relationship varies among the different paints.

Fig. 6 compiles the results of over 200 separate runs of FASSP to show how small of a vehicle subpixel fraction can be detected for the of different paint types as a function of sensor SNR.

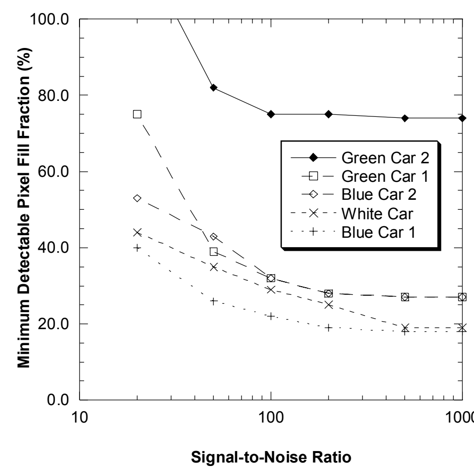

Figure 6. Minimum detectable ($P_D \geq 0.8$ and $P_{FA} \leq 10^{-5}$) pixel fill fraction (%) of the various vehicle paint types as a function of SNR.

We observe in Fig. 6 quite a variation in the minimum detectable subpixel fraction across the various paint types, corresponding to their contrast with the background. However, we also observe that except for the White Car paint, no improvement in the minimum detectable fraction was seen for SNR's higher than 200. While this result is consistent across the scenario studied here, it would not be prudent to generalize this and say no instrument should be built with an SNR greater than 200. There certainly are some applications where a higher SNR can result in a benefit. Examples would be when applying a physics-based atmospheric compensation and the shapes of the atmospheric water vapor absorption bands need to be resolved carefully, or when looking for objects with very specific but subtle spectral features. All the same, this example illustrates a quantifiable method to study such questions in the context of a specific situation.

The last study reported repeats the analysis shown in Fig. 6, except for the Blue Car 2 paint type alone, and studies the effect of number of channels and spectral resolution on the minimum detectable subpixel fraction. The various curves were computed using the indicated number of spectral channels achieved by binning adjacent higher resolution channels by factors of 2, 4, 8, and 16. Again, we see minimal improvement in the minimum detectable fraction with SNR's greater than 200 for the hyperspectral situations, but at the more multispectral-type number of channels and bandwidths, we see little improvement for SNR's greater than 50.

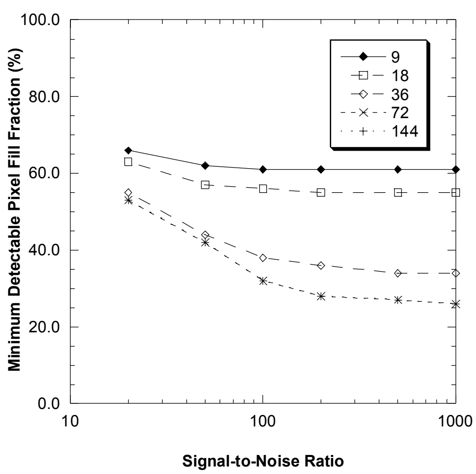

Figure 7. Minimum detectable ($P_D \geq 0.8$ and $P_{FA} \leq 10^{-5}$) pixel fill fraction (%) of the Blue Car 2 vehicle paint type for various number of spectral channels (see text) as a function of SNR.

It is interesting to note that this trend is the opposite of how real instruments work in that for the same integration time and optical design, broader bandwidths would actually achieve higher SNR's. The result in Fig. 7 indicates that higher SNR can be wasted in that it does not further improve the ability of the system to detect objects at smaller subpixel fill fractions for broader multispectral type of sensors.

V. Summary and Discussion

This paper has presented an analytical modeling approach and results for the study of parameter tradeoffs and sensitivities of hyperspectral imaging systems in subpixel object detection applications. While the analytical approach sacrifices the ability to model non-linearities in the remote sensing process, it has the distinct advantage of quick execution (15-30 seconds per run) and the ability to conduct a large number of trade studies in an efficient manner.

Significant conclusions observed in the cases studied here are the dominant impact of target subpixel fill fraction (or equivalently, sensor spatial resolution), the dependence of target to background contrast on detection performance, and the modest (and non-linear) dependence of SNR on target dectectability. Obviously, these trends may indeed be different for other object detection scenarios, but these results illustrate an approach to quantifying the tradeoffs in performance for a variety of top-level system parameters.

References

[1] J.P. Kerekes and D.A. Landgrebe, "An Analytical Model of Earth-Observational Remote Sensing Systems," *IEEE Trans. on Systems, Man, and Cybernetics*, vol. 21, no. 1, pp. 125-133, Jan/Feb 1991.

[2] J.P. Kerekes and D.A. Landgrebe, "Parameter Tradeoffs for Imaging Spectroscopy Systems," *IEEE Trans. on Geosci. and Rem. Sens.*, vol. 29, no. 1, pp. 57-65, January 1991.

[3] J.P. Kerekes and J.E. Baum, "Spectral Imaging System Analytical Model for Subpixel Object Detection," *IEEE Trans. on Geosci. and Rem. Sens.*, vol. 40, no. 5, pp. 1088-1101, May 2002.

[4] J.P. Kerekes and J.E. Baum, "Full Spectrum Spectral Imaging System Analytical Model" *IEEE Trans. on Geosci. and Rem. Sens.*, vol. 43, no. 3, pp. 571-580, March 2005.

[5] J. Kerekes and D. Manolakis, "Improved Modeling of background distributions in an end-to-end spectral imaging system model," *Proceedings of the IEEE International Geoscience and Remote Sensing Symposium (IGARSS'04)*, Anchorage, Alaska, 20-24 September 2004.

[6] J. Kerekes, M. Muldowney, K. Strackerjan, L. Smith, B. Leahy, "Vehicle tracking with multi-temporal hyperspectral imagery," *SPIE Proc. Vol. 6233, Algorithms and Technologies for Multispectral, Hyperspectral, and Ultrapsectral Imagery XII*, Orlando, FL, 17-21 April 2006.

[7] L. Rickard, R. Basedow, E. Zalewski, P. Silverglate, and M. Landers, "HYDICE: An Airborne System for Hyperspectral Imaging," *Proceedings of Imaging Spectrometry of the Terrestrial Environment*, SPIE Vol. 1937, pp. 173-179, 1993.

[8] A. Berk, et al., "MODTRAN Cloud and Multiple Scattering Upgrades with Application to AVIRIS." *Rem. Sens. of Env.*, vol. 65, no. 3, 367-375, September 1998.